



Københavns Universitet



## Microspectroscopy as applied to the study of wood molecular structure

Fackler, Karin; Thygesen, Lisbeth Garbrecht

*Published in:*

Wood Science and Technology

*DOI:*

[10.1007/s00226-012-0516-5](https://doi.org/10.1007/s00226-012-0516-5)

*Publication date:*

2013

*Document Version*

Publisher's PDF, also known as Version of record

*Citation for published version (APA):*

Fackler, K., & Thygesen, L. G. (2013). Microspectroscopy as applied to the study of wood molecular structure. *Wood Science and Technology*, 47(1), 203-222. <https://doi.org/10.1007/s00226-012-0516-5>

# Microspectroscopy as applied to the study of wood molecular structure

Karin Fackler · Lisbeth Garbrecht Thygesen

Received: 19 July 2012 / Published online: 14 December 2012

© The Author(s) 2012. This article is published with open access at Springerlink.com

**Abstract** Microspectroscopy gives access to spatially resolved information on the molecular structure and chemical composition of a material. For a highly heterogeneous and anisotropic material like wood, such information is essential when assessing structure/property relationships such as moisture-induced dimensional changes, decay resistance or mechanical properties. It is, however, important to choose the right technique for the purpose at hand and to apply it in a suitable way if any new insights are to be gained. This review presents and compares three different microspectroscopic techniques: infrared, Raman and ultraviolet. Issues such as sample preparation, spatial resolution, data acquisition and extraction of knowledge from the spectral data are discussed. Additionally, an overview of applications in wood science is given for each method. Lastly, current trends and challenges within microspectroscopy of wood are discussed.

## Introduction

Within the wood science community there is a growing awareness of the link between macroscopic behaviour and the molecular structure within the wood cell wall. It is, however, a challenge to all wood-related research that the anatomical and molecular structure of wood is complex, anisotropic and furthermore depends upon moisture content as well as sample history (i.e., drying-wetting cycles and type and duration of mechanical load). A consequence of the anisotropy on the molecular level is that spatially resolved chemical information is needed in order to understand

---

K. Fackler  
Institute of Chemical Engineering, Vienna University of Technology, Gumpendorfer Straße 1a,  
1060 Vienna, Austria

L. G. Thygesen (✉)  
Faculty of Science, University of Copenhagen, Rømligheidsvej 23, 1958 Frederiksberg C, Denmark  
e-mail: lgt@life.ku.dk

wood and how its intricate structure relates to, for example, moisture absorbance, decay resistance or mechanical properties. These important issues may be addressed using microspectroscopy. Here, three different microspectroscopic techniques are presented: Infrared (IR), Raman and Ultraviolet (UV) microspectroscopy. For more general overviews on these techniques, please refer to Salzer and Siesler (2009) and Šašić and Ozaki (2011). For wood microstructure, many different subjects are addressed using IR, Raman and UV microspectroscopy including wood cell wall formation, architecture and degradation. UV microspectroscopy has been applied to wood and wood products for more than four decades. Successful methods had already been developed around 1970, and sample preparation and equipment usage have remained largely unchanged since then, but advances within data acquisition and processing have made measurements faster and easier with a simultaneous increase in resolution. In recent years, these advances in instrumentation of IR and Raman microspectroscopy for imaging and mapping have opened up many new fields of applications in wood research.

### **Principles of infrared, Raman and UV microspectroscopy with respect to wood analysis**

Basically, all three techniques (IR, Raman and UV) are based on the interaction of light with the investigated material. However, there are fundamental differences in the way they interact with the sample as summarised in Table 1. The individual characteristics of the techniques result in different strong and weak points with regard to the study of wood. Important to note is that UV only detects lignin and aromatics, while IR and Raman in theory can detect all main wood components. A central point is also that fluorescence from lignin poses a problem in Raman spectroscopy of wood. Another important difference is the spatial resolution obtainable. The spatial resolution of a light microscope is ultimately determined by the diffraction of the radiation which implies that it depends on the wavelength of the light and the numerical aperture of the objective (Griffiths 2009). For wood-related applications, this means that selective acquisition of spectra from the cell wall and its different layers or of the cell corners and rays is only possible using either UV–VIS microscopy or Raman microscopy. For overall compositional changes of single fibres, different tissue types or wood modification IR microspectroscopy may also give important information.

#### **Sample preparation in microspectroscopy**

UV–VIS microspectroscopy and IR microscopy rely on the absorption process of the incident light and are therefore often performed in transmission mode, whereas Raman is based on scattered light and has to be performed in reflection. To work in transmission mode, a defined thickness of the sample is necessary, and to work in reflectance mode, a planar surface is required when scanning (imaging) of the samples is aimed at. Therefore, all microspectroscopy relies on proper sample preparation. For UV–VIS transmission experiments, samples of 0.5–1  $\mu\text{m}$  thickness

**Table 1** Characteristics of infrared, Raman and UV microspectroscopy relevant for the study of wood and other types of lignocellulosic biomass

	Infrared	Raman	Ultraviolet
Excitation	Polychromatic Globar IR	Monochromatic Laser UV–VIS–NIR	Polychromatic UV lamp UV–VIS
Principle	Vibrational transition	Vibrational transition	Electronic transition
Spectra	Polar bonds (change in dipole moment), functional groups	Symmetric structures (change in polarizability) molecular backbones	Individual bonds are seldom discernible; spectra consist of wide, non-specific peaks. Only aromatics and conjugated double bonds detectable
Resolution			
Lateral	5–20 $\mu\text{m}$	0.3–2 $\mu\text{m}$	0.25 $\mu\text{m}$
Confocal	Not possible	~2.5 $\mu\text{m}$	Not possible
Sampling modes	Transmission, reflectance, transfectance or attenuated total reflectance (ATR)	Reflectance (scattering)	Transmission
Sample preparation	Optimal thickness (transmission mode) or sample contact (ATR) mode necessary	Plane surface for mapping/imaging, no contact, water as solvent or glass as container do not disturb	Embedding in Epoxy, microtoming 0.5–1 $\mu\text{m}$ thick sections using a diamond knife
Problems	strong absorption of glass, $\text{H}_2\text{O}$ and $\text{CO}_2$	Fluorescence, sample destruction, low S/N	Demanding sample preparation, only some wood components are visible. Glass cannot be used
Frequency range	4,000–700 $\text{cm}^{-1}$	4,000–50 $\text{cm}^{-1}$ (stokes and antistokes)	240–800 nm (12,500–50,000 $\text{cm}^{-1}$ )

are required, whereas samples for IR can be thicker (around 10  $\mu\text{m}$ , in some cases 20–30  $\mu\text{m}$ ). For the very thin cuttings in UV microscopy (typically 1  $\mu\text{m}$ ), the wood is embedded in Spurr's epoxy resin (Spurr 1969). For IR and Raman microscopy also fresh samples can be cut by a rotary or sliding microtome to a thickness between 10 and 20  $\mu\text{m}$ . Fresh samples have the advantage that no signal of the embedding medium shows up in the spectra. The advantage of embedded samples is a flatter surface and the absence of holes in the samples, which can produce artefacts due to changed scattering conditions at the margins. A planar surface is very important for scanning experiments in reflection mode, for example, the Raman imaging approach. Regarding depth resolution, the use of a laser as excitation source in Raman microscopy allows confocal measurements.

## Spectral acquisition and data analysis

All three microspectroscopy methods can be applied in three different modes: point, line or map.

Map acquisition provides a spectroscopic image that can be directly compared to the corresponding visual image. During the last years, mapping has become considerably faster within IR and Raman microscopy, but still the sampling time for acquisition of a complete, high-resolution map comprising several hundreds or thousands of spectra can be very long, even in the range of hours. Long sampling times may pose a problem as drying of the specimen due to heating during the scanning may change both the molecular structure and the physical dimensions of the specimen. This can knock the sample out of focus, may complicate comparison with the visual image and/or make the first and last captured parts of the map incomparable.

The mode of acquisition determines the amount of data captured, and this again affects how the data are analysed. Data from point acquisition and to some extent from line scans are typically assessed manually, that is, qualitative differences and likenesses between the various regions probed are identified from visual inspection of the spectra. For map scans using only a single frequency, this approach is still possible, but for full map acquisitions the amount of data is too large for this approach to be feasible. Chemometric approaches are becoming more and more common, as they allow systematic handling and structuring of large data sets and offer ways of extracting and visualising analysis results (Geladi et al. 2010).

## Infrared, Raman and UV–VIS spectra of wood

### *IR and Raman spectra of wood*

As both methods monitor fundamental vibrational modes, the wavenumber range of the acquired spectra coincides. Raman microscopy records the shift from the excitation wavelength as a full spectrum from 4,000 to around 200  $\text{cm}^{-1}$ , whereas in IR microscopy a narrower range is observed. The small apertures required for IR microspectroscopy with diffraction limited spatial resolution let less photons arrive at the detector. Therefore, the most sensitive detectors of the type narrow band mercury cadmium telluride (MCT) are required, which are only sensitive down to 700  $\text{cm}^{-1}$  (Griffiths 2009). The spectral range of current multichannel focal plane array (FPA) detectors is even smaller (3,600–900  $\text{cm}^{-1}$ ) and excludes prominent wood-related IR bands between 900 and 700  $\text{cm}^{-1}$ .

IR and Raman spectra of wood are characterised by a high number of overlapping bands due to the similar chemical structure of cellulose and hemicelluloses. Consequently, exact band assignment and extraction of chemical and structural information are often challenging. Nevertheless, many assignments of IR and Raman bands related to distinct chemical groups of wood polymers have been available for a long time. Pioneering IR studies of polysaccharides were published in the 1950–1970s (e.g., Liang and Marchessault 1959a, b; Marchessault 1962; Nieduszynski and Marchessault 1972) and for Raman in 1987 (Wiley and

Atalla 1987). The plant polysaccharides group of the Slovak Academy of Sciences (Kačuráková et al. 1994, 1999, 2000) contributed with investigations on the different hemicelluloses, whereas Faix (1991) carried out fundamental work on IR spectroscopy of lignins of different origin. Investigations on reference substances helped a lot in the understanding of Raman spectra of lignin and their resonant enhancement at different laser wavelengths (Larsen and Barsberg 2010; Saariaho et al. 2003; Takayama et al. 1997). Comprehensive band assignments for the whole spectral range are summarised by Agarwal and Ralph (1997) for Raman and by Schwanninger et al. (2004) for IR.

The scientific work on band assignments mostly follows an empirical approach and analyses (partly) purified reference substances. Recent work (Barsberg 2010; Barsberg et al. 2011; Larsen and Barsberg 2010) points towards a novel approach where molecular dynamics contribute to definite assignments of vibrational bands also of complicated polymer compounds such as wood, where extinction coefficients and band positions are highly dependent on the molecular environment.

Besides the chemical composition, IR and Raman microscopy can also reveal important information on the preferred orientation of the wood polymers within the wood fibre. Depending on the angle between the laser polarisation direction and the longitudinal fibre direction, the intensity of certain bands changes considerably. This is due to the orientation of the cell wall polymers, especially the cellulose. In the analysis of spectra, this has to be taken into account and one can even extract orientational information (Gierlinger et al. 2010). By inserting a polarizer in the beam path of the IR microscope, this method can also be used to extract information on the orientation of the wood polymers (Stevanic and Salmén 2009).

In Resonance Raman spectroscopy, the excitation wavelength is tuned to the electronic absorption of the molecule or chromophore which lead to an enhancement of this entity by a factor of up to  $10^6$ . This enables the “visualisation” of the vibrational frequencies within the molecule of interest and effective suppression of unwanted background signal. Intense fluorescence emission associated with complex samples usually occurs in the same spectral region as the resonance Raman spectra and irretrievably swamps weaker Raman signals (Petry et al. 2003). The fluorescence problem can also be circumvented by probing well below the fluorescence emission in the ultraviolet (UV) (Halttunen et al. 2001), an approach that offers also the benefit of a higher signal strength compared to NIR excitation. The UV resonance Raman (UVR) technique was successfully applied to pulp and paper samples (Halttunen et al. 2001; Jääskeläinen et al. 2006; Saariaho et al. 2003, 2004, 2005), heat treated wood (Nuopponen et al. 2004) and for investigations on the photodegradation of lignin (Pandey and Vuorinen 2008).

Some 10 years ago, a fluorescence rejection device was developed (Everall et al. 2001; Matousek et al. 1999, 2001), which effectively suppresses fluorescence background of biological samples (Knorr et al. 2010). This instrument is based on a high throughput optical Kerr shutter separating Raman light from fluorescence in the time domain. Unlike in conventional Raman spectroscopy, the sample is excited using a high repetition rate (kHz) picosecond laser pulse (1 ps). Due to the instantaneous nature of Raman scattering, the Raman signal is emitted first from the sample with fluorescence emitted on a substantially longer timescale (typically

nanoseconds). The two signals are thus effectively separated. By use of the Kerr gate, the fluorescence background of chemical pulp samples excited with a 400-nm excitation line was suppressed effectively (Saariaho et al. 2004). Kerr gated resonance Raman spectroscopy enabled (Barsberg et al. 2005) to elucidate lignin structures with unique sensitivity and selectivity and for the first time to study lignin radicals as crucial intermediates for lignin biosynthesis in wood cell walls (Barsberg et al. 2006).

### UV–VIS spectra of lignin and other ring structures

The main lignin UV absorbance peak is found around 280 nm and depends upon the delocalised  $\pi$  electron system in the aromatic rings (Kleist and Bauch 2001). The position and the intensity of this peak reflect the contents of the different monomers within the lignin, that is, syringyl (S, two methoxyl (MeO) groups per aromatic ring), guaiacyl (G, one MeO group per ring) and p-hydroxyphenyl (H, no MeO groups on the ring). UV spectra of model compounds presented by Musha and Goring (1975) show that G has its maximum absorbance around 280–285 nm, S approximately at 270–275 nm and H at 255–260 nm (Fig. 1). These differences in absorbance maximum between lignin units imply that a wavelength of 280 nm is well suited for lignin mapping in softwoods as they normally contain only guaiacyl. For hardwoods and monocots that usually contain both syringyl and guaiacyl, a slightly shorter wavelength may be more suitable.

Decreasing intensity is seen for an increasing number of MeO groups per monomer. According to the extinction coefficients for G and S as calculated by Fergus and Goring (1969, 1970b), the absorbance of G at 280 nm should be

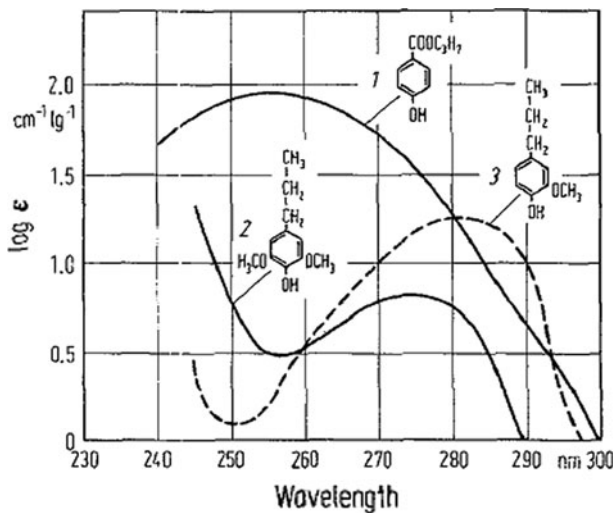


**Fig. 1** UV spectra of lignin model compounds. Spectra of guaiacyl (Aulin-Erdtman 1953), syringyl (Pew 1962) and p-hydroxy (Lang 1963) model compounds. Reproduced from Musha and Goring (1975) with permission from Springer

approximately three times higher than for S. However, as shown by Goldschmid (1976), both the absorbance levels and the peak positions of H, G and S derivatives vary considerably depending on the derivative and whether it is ionised or not. Direct transfer of information based on lignin model substances to native or processed lignin is thus not reasonable.

A broad absorbance range of native wood may be found to the right of the 280 peak, that is, at longer wavelengths. Absorbance both in the 280-nm region and above is ascribed to the presence of chromophoric groups such as conjugated double bonds attributed to highly condensed phenolics (Koch et al. 2003). A higher degree of conjugation is known to stabilize  $\pi - \pi^*$  transitions resulting in a bathochromic shift of the UV absorbance, that is, a shift towards longer wavelengths (Goldschmid 1976). A long absorbance shoulder above 280 nm may or may not be found for wood depending on species, tissue type and treatment (if any) (Adamopoulos and Koch 2011; Koch et al. 2003).

UV absorbance spectra and maps convey qualitative chemical differences between different morphological regions, that is, cell types and/or tissue types (Musha and Goring 1975). Like for other types of microscopy, semi-quantitative or even quantitative comparisons (such as for example lignin content) require the use of reference methods as well as strict standardization and usually also some form of normalisation of the spectral information and/or the use of chemometric tools. As UV spectra from wood consist of broad and overlapping composite peaks, quantification attempts should be carried out with caution, as peaks may contain absorbencies unrelated to the topochemical information of interest. Peaks due to non-lignin polyphenols may for example overlap with lignin (Kleist and Bauch 2001; Watanabe et al. 1997, 2004).

### **Application of microspectroscopy within the study of wood molecular structure**

Microspectroscopy has been applied to several subjects within the study of wood molecular structure. Here, examples from three main subject areas are presented: (1) cell wall biochemical composition, architecture and formation, (2) cell wall polymer orientation and (3) cell wall degradation.

#### **Cell wall biochemical composition, architecture and formation**

Despite the limited spatial resolution, early FT-IR microspectroscopy work by Kataoka and Kondo (1996) revealed the relative distribution of cellulose crystal allomorphs  $I_\alpha$  and  $I_\beta$  in wood cell walls and provided in vivo evidence that the major crystalline component of cellulose changes from  $I_\alpha$  to  $I_\beta$  when the enlarging growth of coniferous cells ceases. Primary tracheid cell walls were enriched in cellulose  $I_\alpha$ , whereas cellulose  $I_\beta$  dominated in secondary cell walls. In a later paper, the same authors (Kataoka and Kondo 1998) were able to confirm that stress-induced crystallisation leads to formation of cellulose  $I_\alpha$ , which is oriented to a lesser extent along the tracheid direction than cellulose  $I_\beta$  of secondary cell walls. In this first polarisation IR microspectroscopy study of wood, the intensity of the band of the



glycosidic bond of cellulose at  $1,160\text{ cm}^{-1}$  indicated cellulose orientation, as its vibration is oriented parallel to the cellulose main chains. Its band height was highly dependent on the polarisation angle of the IR radiation, which allowed for conclusions on the orientation of cellulose microfibrils within the different cell wall regions. Applying validated cellulose crystallinity indices, it was furthermore proposed that cellulose of  $I_{\alpha}$  enriched primary cell walls exhibits higher crystallinity than cellulose of  $I_{\beta}$  enriched secondary cell walls. These findings were (partly) confirmed by Labbé et al. (2005), who could rely on a much higher number of spectra gained through an IR imaging system in  $6.25\text{ }\mu\text{m}$  spatial resolution. The different molecular structure and chemical composition allowed for predicting the distance between the position and the cambial zone using partial least squares regression.

The hydrogen bonding within a single spruce tracheid at different ambient conditions—in air, in deuterium oxide and in dimethylacetamide was studied by Schmidt et al. (2006). The authors used synchrotron radiation coupled into the IR microscope and carried out polarised (linear dichroism) IR measurements with a polarisation modulation module. The technique allowed the observation of cellulose crystal allomorphs and gave information on hydrogen bonding, orientation and ordering of submolecular groups, and on the accessibility of the various OH groups to the solvents dimethylacetamide (DMAc) and deuterium oxide ( $\text{D}_2\text{O}$ ). O–H groups of cellulose exhibiting strong intramolecular H-bonds were confirmed to be oriented parallel to the fibre axis. These OH groups were not accessible to DMAc and  $\text{D}_2\text{O}$ , whereas O–H groups with parallel and perpendicular orientation relative to molecules in amorphous or less ordered regions of the fibre cell walls were more accessible.

Chemical images obtained by IR microscopy demonstrated the distribution of lignin and polysaccharides within cross sections of beech and poplar wood and the spatial distribution of G/S lignin ratios (Müller and Polle 2009; Naumann and Polle 2006). The authors could resolve the lignin enriched middle lamellae and detected relative enrichment of G-lignin in the walls of vessels. Burgert et al. (2005) investigated the chemical differences between chemically and mechanically isolated single spruce wood fibres. They found extensive degradation of the lignin component and suggestions of a slight hemicelluloses breakdown in the fibres isolated with a chemical maceration method in the presence of hydrogen peroxide and glacial acetic acid. Differences of the relative concentrations of wood components within cross sections of whole stems of a one-year-old poplar (*Populus trichocarpa*) were investigated by Gou et al. (2008). They proposed the enrichment of aromatics within the cortex, found more proteins in the phloem, whereas polysaccharides, including acetylated polysaccharides, were mainly observed in the woody tissue (vascular xylem). The low level of lignin in the young poplar stems was deposited among vascular tissues. Gorzsás et al. (2011) used imaging FT-IR microspectroscopy combined with a multivariate approach to identify, characterise and to visualise different chemotypes of the secondary xylem cell types of *Populus tremula*. This not only allowed the differentiation and allocation of spectra to different cell types (vessels, early- and latewood fibres, and terminal axial parenchyma) but also revealed the differences in chemistry between the secondary xylem among the investigated cell types related to their lignin and cellulose contents.

Early Raman microprobe spectroscopy showed that lignin as well as cellulose can be studied in the native cell walls (Agarwal and Atalla 1986). Within the middle lamella, heterogeneity of lignin concentration was shown (Tirumalai et al. 1996). Deposits in differentiating tracheids were investigated selectively and showed similar spectra to that of coniferin (Morikawa et al. 2010). To obtain a better understanding of heartwood formation, FT-(NIR) Raman spectroscopy was applied to measure the changes in pino-sylvin content in the transition zone between sapwood and heartwood of Scots pine (*Pinus sylvestris* L.) (Bergström 2003; Bergström et al. 1999). No seasonal pattern in the concentration was found, indicating that heartwood formation was not linked to a specific time of the year. In another study by Osterberg et al. (2006), precipitated wood extractives were detected on cellulose fibres using a combined atomic force microscope (AFM) and confocal Raman microscope, which made it possible to obtain morphological and chemical information from the same location within the sample.

During the last 5 years or so, Raman mapping of selected areas and calculating chemical images based on the changes in the Raman spectra has become popular (Agarwal 2006; Gierlinger and Schwanninger 2006). The images reveal the distribution of the wood polymers on the  $\mu$ -level in the native cell wall. However, the angle between laser polarisation direction and cellulose microfibril orientation has a big influence on the band intensity of most of the vibrations attributed to cellulose (Atalla et al. 1980). Therefore, care has to be taken to proper sample and laser alignment and not to mix up changes in content with changes in orientation (Gierlinger and Schwanninger 2006). Lignin, which is less oriented than cellulose within the wood cell wall (Stevanic and Salmén 2009; Gierlinger et al. 2010), can be mapped by having marker bands not overlapping with contributions from cellulose and hemicelluloses. Even small amounts in a very thin layer towards the lumen of G-layer of poplar tension wood could be visualised (Agarwal 2006). The different lignification of tension wood was visualised in Raman images of maple (*Acer* spp.), beech (*Fagus sylvatica*) and oak (*Quercus robur*) (Lehringer et al. 2008). Schmidt et al. (2009) studied the lignification in wild-type and lignin-reduced 4CL transgenic *Populus trichocarpa* stem wood and showed that transgenic reduction of lignin is particularly pronounced in the S2 wall layer of fibres (Schmidt et al. 2009).

A group of UV microspectroscopy studies report on differences and likenesses in lignin content and type within and between different cell types or tissue types. The pioneering works within this line of research were carried out around 1970 and include Fergus et al. (1969) who used UV microspectroscopy to measure higher lignin contents in cell corners and middle lamella than in the secondary wall of black spruce (*Picea mariana*), Bland and Hillis (1969) who explored different UV wavelengths for mapping lignin and polyphenols in Radiata pine (*Pinus radiata*) and other species and Fergus and Goring (1970a, b) who mapped the content and type of lignin in white birch (*Betula papyrifera*) and found that the lignin in vessel cell walls contained mostly guaiacyl units, while fibre walls contained more syringyl units. Later papers focussing on differences between cell types or tissue types include Yoshinaga et al. (1997), who studied Japanese oak (*Quercus mongolica*) and also found that the proportion of syringyl units tended to increase as cell functions changed from water conductivity to mechanical support. Further, they

found that the tips of xylem cells were richer in syringyl units than the middle part of the cells. Watanabe et al. (2004) found that also for two Eucalyptus species were fibre cell walls richer in syringyl units than vessel cell walls. Jungnikl et al. (2008) looked for a possible correlation between cellulose microfibril angle and lignin content in the S<sub>2</sub> layer, but did not find such a correlation.

UV microspectroscopy has also been used for studies concerning xylem formation and lignification processes within the living tree. Work along this line includes studies of the deposition of cell wall components during the differentiation of xylem cells in normal and 35S-*rolC* transgenic hybrid aspen *Populus tremula* × *P. tremuloides*, (Dünisch et al. 2006; Grünwald et al. 2001, 2002a, b), which has a dwarfed phenotype. In the wild-type, polysaccharides were deposited before the lignin during cell wall formation, while these two events proceeded more in parallel in the transgenic plants. In another set of studies, Schmitt et al. (2003) and Gricar et al. (2005) studied the cell wall structure of terminal latewood tracheids from both healthy and declining silver fir trees (*Abies alba*). It was found that healthy trees and trees with relatively broad growth rings continued secondary cell wall formation and lignification longer in the autumn than declining trees and trees with narrow rings. Prislan et al. (2009) studied the developing xylem of beech (*Fagus sylvatica*). Among other observations, it was found that cell differentiation continued about 4 weeks after cambial cell divisions had stopped and that in the lignin of this terminal xylem, the guaiacyl content increased in fibres, while the syringyl content increased in vessels, which is in contrast to the results of Fergus and Goring (1970a) concerning the identity of the monolignols present in the cell walls of fibres and vessels in hardwoods.

A group of UV studies have concerned tension wood in various hardwood species (Lehringer et al. 2008; Ruelle et al. 2007; Yoshida et al. 2002; Yoshizawa et al. 2000) and have shown a decrease in absorbance around 280 nm corresponding to a decrease in lignin content (G units). One study has taken a more intervening experimental approach to UV studies of tension wood (Yoshida et al. 2005) by inducing extra gravity to growing secondary xylem of *Prunus jamasakura*. The study showed that while the overall lignin content decreased, the lignin content in fibres increased compared to control specimens. For compression wood in Norway spruce, Gindl (2002) found an increase in lignin content in the S<sub>2</sub> layer and a decrease in the ratio between absorbance at 280 and 260 nm, corresponding to an increase in the content of P units.

### Cell wall polymer orientation

Polarised vibrational spectroscopy can be used to investigate the cell wall polymer orientation as the absorbance is larger of bands oriented nearly parallel (i.e. <45°) to the polarisation direction than when the same bands are oriented nearly orthogonal (i.e. >45°) to the polarisation direction.

Stevanic and Salmén (2009) investigated the orientation of all major wood polymers (cellulose, glucomannan, xylan and lignin) within spruce wood fibres using polarisation IR microscopy and found dichroic effects for all of them (Fig. 2a). Several marker bands were assigned to each of the polymers. From their

relative absorbance, the direction of the corresponding molecular vibration and from considerations concerning the molecular structure, the orientation of the polymers within the fibre—mainly assigned to that within the secondary wood cell wall—was concluded. In secondary cell walls, hemicelluloses were found to be oriented along the fibre direction following the principal direction of cellulose microfibrils. For lignin, a lower extent of orientation was found (Fig. 2b).

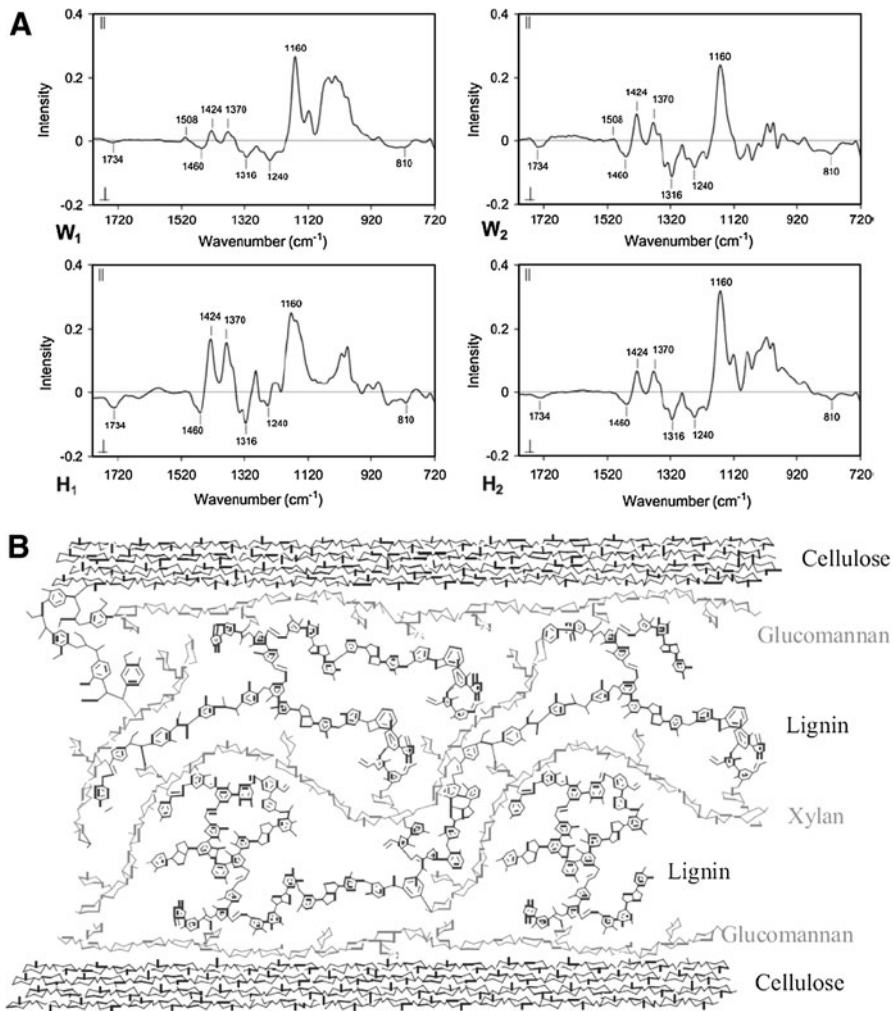


**Fig. 2** **a** Average orientation spectra of two wood fibres ( $W_1$  and  $W_2$ ) and two holocellulose fibres ( $H_1$  and  $H_2$ ), respectively. In each spectrum, specific absorption peaks related to the different wood polymers are indicated, viz. cellulose 1,160, 1,316, 1,370 and 1,424  $\text{cm}^{-1}$ , glucomanan 810  $\text{cm}^{-1}$ , xylan 1,734, 1,460 and 1,240  $\text{cm}^{-1}$  and lignin 1,508  $\text{cm}^{-1}$ . Reproduced from Stevanic and Salmén (2009) with permission from De Gruyter. **b** Orientation of polysaccharides and lignin on the molecular level in a model of an S2 cell wall layer based on the studies by Salmén and coworkers. Reproduced from Henriksson (2009) with permission from De Gruyter

With a similar approach of polarisation FT-IR, the cell wall architecture of hybrid aspen wood (normal wood and tension wood) was elucidated (Olsson et al. 2011). Also hardwood cell walls follow a highly organised and oriented structural pattern with the xylan and lignin showing an even higher degree of orientation along the fibre direction than in softwoods. In the gelatinous (G) layers of tension wood, ester groups associated with xylan oriented perpendicularly to the direction in normal wood were observed. It was proposed that these ester groups are linked to other sugar units that interfere with the xylan signal in tension wood. Furthermore, in this paper, polarisation FTIR spectroscopy was proposed to estimate the microfibrillar angle (MFA) in crude approximation. MFA of tension wood was confirmed to be lower than that of normal wood. The extent of lignin and cellulose orientation assessed with polarisation FT-IR microscopy within different wood species is highly dependent on the cell wall region (Salmén et al. 2012). Whereas secondary cell walls follow a highly oriented anisotropic order along the cellulose microfibrils to which also lignin contributes, middle lamella lignin can be considered completely isotropic.

It was polarised Raman microscopy that showed, for the first time, that the phenyl rings of secondary cell wall lignin most often are oriented in the plane of the cell wall (Atalla and Agarwal 1985). For cellulose, different orientation of the microfibrils within the different cell wall layers (S2, S1) and cell types are known and can be visualised with the Raman imaging approach (Gierlinger and Schwanninger 2006). A detailed study of the intensity change of the cellulose bands in context with the angle between laser polarisation direction and cellulose microfibril angle allowed the determination of the microfibril angle of compression, opposite and normal spruce wood (Gierlinger et al. 2010).

### Cell wall degradation

Spatial variation of wood chemistry and structure is a common feature of wood degradation. The earliest paper on microspectroscopy of wood modification/degradation was published by Kataoka and Kiguchi (2001) who analysed UV photodegradation of wood using IR microspectroscopy. Like in the above described study on cell wall formation (Kataoka and Kondo 1996), a microspectroscopy system with a measuring spot of  $50\text{T} \times 200\text{L} \mu\text{m}^2$  in size was employed and the ratio between carbonyl groups ( $1,730 \text{ cm}^{-1}$ ) and aromatic rings ( $1,510 \text{ cm}^{-1}$ ), which are both highly affected by UV irradiation indicated the depth of photo-induced degradation of wood. In a later study (Kataoka et al. 2007), it was demonstrated that the depth of photo-induced degradation increased with increasing wavelength up to and including violet visible light.

The effect of steam treatment on the properties of wood cell walls was investigated by Yin et al. (2011). Randomly selected FT-IR spectra from clear secondary cell wall areas identified from FT-IR absorbance images were analysed and revealed the progressive degradation of carbonyl groups, the decomposition of the glucomannan backbone and the loss of carbonyl groups of lignin. These chemical changes were put into context with changes on moisture sorption and indentation modulus, a micromechanical property.

A very powerful example on the potential of FT-IR imaging as a tool to characterise structural and chemical changes of wood, to propose and characterise degradation kinetics during pyrolysis of wood and to visualise these characteristics as chemical images was provided by (Bahng et al. 2011). Spectral changes were assigned to the well-known decomposition of hemicelluloses leading to the formation of acid groups followed by condensation reactions, tar formation and finally char formation.

Fackler et al. (2010) characterised and localised wood degradation caused by brown rot fungi within spruce wood and provided the first work on multivariate analysis of IR microscopic images from wood (Fig. 3). Most indicative for early brown rot was the cleavage of glycosidic bonds of polysaccharides prior to their metabolisation in middle lamellae, primary cell walls or outer secondary cell walls. In more pronounced degradation stages, lignin accumulation due to the selective degradation of polysaccharides took place. In a similar way, spruce wood degraded by a simultaneous and a selective white rot fungus was analysed (Fackler et al. 2011). Cleavage of glycosidic bonds was also indicative for simultaneous white rot degradation, albeit to a much lesser extent than for early brown rot while selective white rot could be detected due to the reduction of the lignin content of spruce wood. White rot decay was shown to be evenly distributed within secondary cell walls of tracheids.

Gierlinger et al. (2008) used Raman microspectroscopy to study in situ enzymatic degradation of poplar wood cell walls within a custom-built fluidic cell. They found that as the set-up continuously provided fresh highly concentrated cellulases, cellulose accessibility was the limiting factor and thus the G-layers of tension wood were degraded considerably faster than normal wood cell walls.

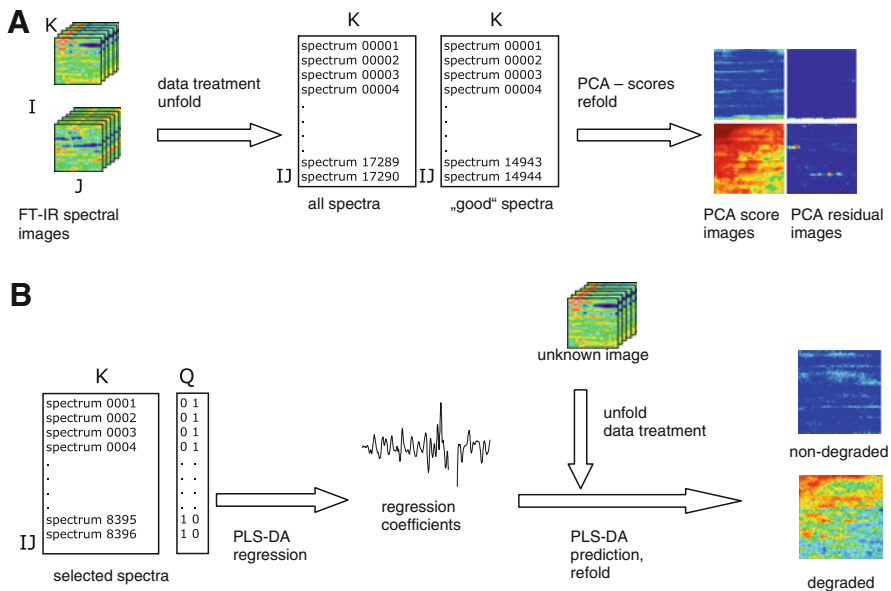


**Fig. 3** Approaches to multivariate image analysis (MIA) for visualisation of brown rot degradation **a** PCA based MIA; **b** PLS-DA based MIA for classification of unknown spectra. Reproduced from Fackler et al. (2010) with permission from Elsevier (colour figure online)



Frankenstein et al. (2006) used UV microscopy to study the effect of wounding on the lignin in the xylem of poplar (*Populus* spp.). A topochemical analysis of the surrounding tissue during the compartmentalisation process was carried out up to 95 weeks after the wounding. It was found that xylem cells near the wounding developed thicker and more lignin rich cell walls. Singh et al. (2006) found that ray tracheids of *Pinus radiata* had cell walls with a higher lignin concentration than the cell walls of axial tracheids, and that the ray tracheids were more resistant against soft rot. This finding suggests that the wound response found by Frankenstein et al. (2006) could help protect the wounded tree from fungal degradation. In another study, Baum et al. (2000) studied the effects of fungal infection (by *Ustulina deusta*) on the G-layer within beech tension wood fibres in the reaction zone and found that this made the tree infiltrate the G-layer with poly phenolics, presumably as a means of protection. Kleist and Schmitt (2001) characterised the decay pattern caused by *Coniophora puteana* in Sapelli wood (*Entandrophragma cylindricum*) and found no lignin degradation in the vicinity of the cell wall cavities caused by the fungi. Blanchette et al. (1997) used UV microspectroscopy to show loss of lignin within the cell walls of loblolly pine wood chips (*Pinus taeda*) decayed by the white rot fungus *Ceriporiopsis subvermispora*. Koch et al. (1996) used UV microspectroscopy to study cell wall degradation in wind-damaged stems of stressed Norway spruce trees (*Picea abies*) and found that the lignin concentration decreased when the trees were infected by the fungi *Stereum sanguinolentum*. Kim et al. (2008) studied weathered pine wood (*Pinus* spp.) and found that the lignin content decreased from the outside of tracheids towards the lumen, and that the middle lamella was highly degraded. In another study, Cufar et al. (2008) used UV microspectroscopy to study the topochemistry of water-logged archaeological wood (oak and ash, *Quercus* spp. and *Fraxinus* spp.) and found that the middle lamella and cell corners were the best preserved parts.

### Current and future trends and challenges

Two key issues within microspectroscopy are the spectral and the spatial resolution that can be obtained. High signal-to-noise ratio and data acquisition times are related to these issues. Therefore, progress within microspectroscopy of wood is basically instrumentation driven. Regarding spatial resolution, IR instruments have already reached the diffraction limit. Because of the shorter wavelengths used, UV microspectroscopy offers better resolution, but allows only lignin and other aromatic compounds to be studied. Furthermore, peaks from the different lignin units and other aromatic phenols are broad and coincide or overlap, making assignments of peaks and peak shifts difficult. Also, as the absorbencies of these substances are different and vary with the wavelength, UV measurements are all in all qualitative in nature, semi-quantitative at best. It seems that Raman microspectroscopy at present offers the best combination of spatial and spectral resolution, with information obtainable at the sub-cell wall level for all three major wood cell wall polymers. The spatial resolution can be driven below the diffraction limit by tip enhanced Raman microscopy (Domke and Pettinger 2010; Stadler et al. 2010).

However, Raman spectroscopy suffers from an inherent low signal-to-noise ratio as well as the problem of fluorescence from lignin and other aromatic compounds. Kerr gated Raman or the use of NIR lasers may circumvent this problem, but at the cost of even lower signal-to-noise ratios.

A trend that seems to be emerging is the in situ use of microspectroscopy, that is, measurements that take place while the specimen is undergoing some change or treatment (e.g. mechanical stress). However, for these applications, the acquisition time poses a problem in some situations, especially for imaging applications where the acquisition time for a single image at present can easily be hours. This precludes many applications. Here, further progress in instrumentation (detector sensitivity) might lead to faster acquisition times, which will make it possible to follow also processes with shorter time scales.

The selectivity of the spectral information captured also needs to be addressed. In future studies, interactions of light with wood and fibre structures causing effects other than the excitation of molecular vibrations or electronic transitions will have to be taken into account to a higher extent. Light scattering and effects due to heterogeneity within samples not only lead to loss of spatial information but may also cause band shifts. The latter effect due to resonant Mie scattering is typically observed on very small objects and sample margins (Bassan et al. 2009; Davis et al. 2010, 2011).

Once spectra of an acceptable quality have been captured, the problems are not over. What has to be considered when fancying imaging microscopy is the amount of data one has to deal with. Despite its undisputed powerfulness, extracting structural and chemical information and visualising the data in an appropriate way is challenging and at present requires a lot of manual work due to the current lack of comprehensive spectroscopy and imaging software tools. Furthermore, spectral differences within biological samples are usually very small and univariate approaches of data analysis sometimes reveal only a share of the exploitative information contained in the spectra making chemometrics an important tool in many cases

**Acknowledgments** The authors thank Dr. Notburga Gierlinger for substantial contributions to this paper. The Austrian Science Fund (Project Number V117-N17 granted to K. F.) is gratefully acknowledged. This review is based on the development of fundamental knowledge within the network of COST Action FP0802 “Experimental and computational microcharacterisation techniques in wood mechanics” during the years 2008–2012. The authors are grateful to the support from the European Science Foundation through COST and to all scientists contributing to the development work in this network. In addition, K. F. acknowledges the support by the Austrian Science Fund—FWF (Project number V117-N17).

**Open Access** This article is distributed under the terms of the Creative Commons Attribution License which permits any use, distribution, and reproduction in any medium, provided the original author(s) and the source are credited.

## References

- Adamopoulos S, Koch G (2011) Wood structure and topoxchemistry of *Juniperus excelsa*. Iawa J 32(1):67–76
- Agarwal UP (2006) Raman imaging to investigate ultrastructure and composition of plant cell walls: distribution of lignin and cellulose in black spruce wood (*Picea mariana*). Planta 224(5):1141–1153



- Agarwal UP, Atalla RH (1986) In situ Raman microprobe studies of plant-cell walls—macromolecular organization and compositional variability in the secondary wall of *Picea mariana* (Mill) Bsp. *Planta* 169(3):325–332
- Agarwal U, Ralph S (1997) FT-Raman spectroscopy of wood: identifying contributions of lignin and carbohydrate polymers in the spectrum of black spruce (*Picea mariana*). *Appl Spectrosc* 51:1648–1655
- Atalla RH, Agarwal UP (1985) Raman microprobe evidence for lignin orientation in the cell walls of native woody tissue. *Science* 227:636–638
- Atalla RH, Whitmore RE, Heimbach CJ (1980) Raman spectral evidence for molecular orientation in native cellulosic fibers. *Macromolecules* 13(6):1717–1719
- Aulin-Erdtman G (1953) Spectrographic contributions to lignin chemistry III. Investigations on model compounds. *Svensk Papperstidning* 56:91–101
- Bahng M-K, Donohue BS, Nimlos MR (2011) Application of an Fourier transform-infrared imaging tool for measuring temperature or reaction profiles in pyrolyzed wood. *Energy Fuels* 25:370–378
- Barsberg S (2010) Prediction of vibrational spectra of polysaccharides—simulated IR spectrum of cellulose based on density functional theory (DFT). *J Phys Chem B* 114(36):11703–11708
- Barsberg S, Matousek P, Towrie M (2005) Structural analysis of lignin by resonance Raman spectroscopy. *Macromol Biosci* 5(8):743–752
- Barsberg S, Matousek P, Towrie M, Jorgensen H, Felby C (2006) Lignin radicals in the plant cell wall probed by Kerr-gated resonance Raman spectroscopy. *Biophys J* 90(8):2978–2986
- Barsberg S, Sanadi AR, Jorgensen H (2011) A new density functional theory (DFT) based method for supporting the assignment of vibrational signatures of mannan and cellulose—analysis of palm kernel cake hydrolysis by ATR-FT-IR spectroscopy as a case study. *Carbohydr Polym* 85(2):457–464
- Bassan P, Byrne HJ, Bonnier F, Lee J, Dumas P, Gardner P (2009) Resonant Mie scattering in infrared spectroscopy of biological materials—understanding the dispersion artefact. *Analyst* 134:1586–1593
- Baum S, Schwarze F, Fink S (2000) Persistence of the gelatinous layer within altered tension-wood fibres of beech degraded by *Ustilina deusta*. *New Phytol* 147(2):347–355
- Bergström B (2003) Chemical and structural changes during heartwood formation in *Pinus sylvestris*. *Forestry* 76(1):45–53
- Bergström B, Gustafsson G, Gref R, Ericsson A (1999) Seasonal changes of pinosylvyn distribution in the sapwood/heartwood boundary of *Pinus sylvestris*. *Trees Struct Funct* 14:65–71
- Blanchette RA, Krueger EW, Haight JE, Akhtar M, Akin DE (1997) Cell wall alterations in loblolly pine wood decayed by the white-rot fungus, *Ceriporiopsis subvermispora*. *J Biotechnol* 53(2–3):203–213
- Bland DH, Hillis WE (1969) Microspectrophotometric investigation of lignin and polyphenol distribution in wood sections. *Appita* 23(3):204–210
- Burgert I, Gierlinger N, Zimmermann T (2005) Properties of chemically and mechanically isolated fibres of spruce (*Picea abies* [L.] Karst.). Part 1: structural and chemical characterisation. *Holzforschung* 59:240–246
- Cufar K, Gricar J, Zupancic M, Koch G, Schmitt U (2008) Anatomy, cell wall structure and topochemistry of water-logged archaeological wood aged 5,200 and 4,500 years. *Iawa J* 29(1):55–68
- Davis BJ, Carney PS, Bhargava R (2010) Theory of mid-infrared absorption microspectroscopy: II. Heterogeneous samples. *Anal Chem* 82:3487–3499
- Davis BJ, Carney PS, Bhargava R (2011) Theory of infrared microspectroscopy for intact fibers. *Anal Chem* 83:525–532
- Domke KF, Pettinger B (2010) Studying surface chemistry beyond the diffraction limit: 10 years of TERS. *Chem Phys Chem* 11:1365–1373
- Dünisch O, Fladung M, Nakaba S, Watanabe Y, Funada R (2006) Influence of overexpression of a gibberellin 20-oxidase gene on the kinetics of xylem cell development in hybrid poplar (*Populus tremula* L. and *P. tremuloides* Michx.). *Holzforschung* 60(6):608–617
- Everall N, Hahn T, Matousek P, Parker AW, Towrie M (2001) Picosecond time-resolved Raman spectroscopy of solids: capabilities and limitations for fluorescence rejection and the influence of diffuse reflectance. *Appl Spectrosc* 55(12):1701–1708
- Fackler K, Stevanic JS, Ters T, Hinterstoisser B, Schwanninger M, Salmén L (2010) Localisation and characterisation of incipient brown-rot decay within spruce wood cell walls using FT-IR imaging microscopy. *Enzyme Microb Technol* 47:257–267

- Fackler K, Stevanic JS, Ters T, Hinterstoisser B, Schwanninger M, Salmén L (2011) FT-IR imaging microscopy to localise and characterise simultaneous and selective white-rot decay within spruce wood cells. *Holzforschung* 65:411–420
- Faix O (1991) Classification of lignins from different botanical origins by FTIR spectroscopy. *Holzforschung* 45(Supplement):21–27
- Fergus BJ, Goring DAI (1969) Topochemistry of delignification in Kraft and neutral sulphite pulping of birch wood. *Pulp Paper Can* 70(18):65–73
- Fergus BJ, Goring DAI (1970a) Distribution of lignin in birch wood as determined by ultraviolet microscopy. *Holzforschung* 24(4):118–124
- Fergus BJ, Goring DAI (1970b) Location of guaiacyl and syringyl lignins in birch xylem tissue. *Holzforschung* 24(4):113–117
- Fergus BJ, Procter AR, Scott JAN, Goring DAI (1969) Distribution of lignin in sprucewood as determined by ultraviolet microscopy. *Wood Sci Technol* 3(2):117–138
- Frankenstein C, Schmitt U, Koch G (2006) Topochemical studies on modified lignin distribution in the xylem of poplar (*Populus* spp.) after wounding. *Ann Bot* 97(2):195–204
- Geladi P, Grahn H, Manley M (2010) Data analysis and chemometrics for hyperspectral Imaging. In: Sasic S, Ozaki Y (eds) Raman, infrared, and near-infrared chemical imaging. Wiley, Hoboken, pp 93–109
- Gierlinger N, Schwanninger M (2006) Chemical imaging of poplar wood cell walls by confocal Raman microscopy. *Plant Physiol* 140:1246–1254
- Gierlinger N, Goswami L, Schmidt M, Burgert I, Coutand C, Rogge T, Schwanninger M (2008) In situ FT-IR microscopic study on enzymatic treatment of poplar wood cross-sections. *Biomacromolecules* 9(8):2194–2201
- Gierlinger N, Luss S, König C, Konnerth J, Eder M, Fratzl P (2010) Cellulose microfibril orientation of *Picea abies* and its variability at the micron-level determined by Raman imaging. *J Exp Bot* 61(2):587–595
- Gindl W (2002) Comparing mechanical properties of normal and compression wood in Norway spruce: the role of lignin in compression parallel to the grain. *Holzforschung* 56(4):395–401
- Goldschmid O (1976) Ultraviolet spectra. In: Sarkanen KV, Ludwig CH (eds) Lignins: occurrence, formation, structure and reactions. Wiley, New York, pp 241–266
- Gorzás A, Stenlund H, Persson P, Trygg J, Sundberg B (2011) Cell-specific chemotyping and multivariate imaging by combined FT-IR microspectroscopy and orthogonal projections to latent structures (OPLS) analysis reveals the chemical landscape of secondary xylem. *Plant J* 66(5):903–914
- Gou J-Y, Park S, Yu X-H, Miller LM, Liu C-J (2008) Compositional characterization and imaging of “wall-bound” acylesters of *Populus trichocarpa* reveal differential accumulation of acyl molecules in normal and reactive woods. *Planta* 229:15–24
- Grigar J, Cufar K, Oven P, Schmitt U (2005) Differentiation of terminal latewood tracheids in silver fir during autumn. *Ann Bot* 95(6):959–965
- Griffiths PR (2009) Infrared and Raman instrumentation for mapping and imaging. In: Salzer R, Siesler HW (eds) Infrared and Raman spectroscopic imaging. Wiley, Weinheim, pp 3–64
- Grünwald C, Ruel K, Joseleau JP, Fladung M (2001) Morphology, wood structure and cell wall composition of roC transgenic and non-transformed aspen trees. *Trees Struct Funct* 15(8):503–517
- Grünwald C, Ruel K, Kim YS, Schmitt U (2002a) On the cytochemistry of cell wall formation in poplar trees. *Plant Biol* 4(1):13–21
- Grünwald C, Ruel K, Schmitt U (2002b) Differentiation of xylem cells in roC transgenic aspen trees—a study of secondary cell wall development. *Ann Forest Sci* 59(5–6):679–685
- Haltunen M, Vyörykkä J, Hortling B, Tamminen T, Zimmermann A, Vuorinen T (2001) Study of residual lignin in pulp by UV resonance Raman spectroscopy. *Holzforschung* 55:631–638
- Henriksson G (2009) Lignin. In: Ek M, Gellerstedt G, Henriksson G (eds) Wood chemistry and wood biotechnology. Pulp and paper chemistry and technology, vol 1. De Gruyter, Berlin
- Jääskeläinen AS, Saariaho AM, Vyörykkä J, Vuorinen T, Matousek P, Parker AW (2006) Application of UV-Vis and resonance Raman spectroscopy to study bleaching and photoyellowing of thermomechanical pulps. *Holzforschung* 60(3):231–238
- Jungnickl K, Koch G, Burgert I (2008) A comprehensive analysis of the relation of cellulose microfibril orientation and lignin content in the S2 layer of different tissue types of spruce wood (*Picea abies* (L.) Karst.). *Holzforschung* 62(4):475–480

- Kačuráková M, Ebringerová A, Hirsch J, Hromádková Z (1994) Infrared study of arabinoxylans. *J Sci Food Agric* 66:423–427
- Kačuráková M, Wellner M, Ebringerová A, Hromádková Z, Wilson RH, Belton BS (1999) Characterisation of xylan-type polysaccharides and associated cell wall components by FT-IR and FT-Raman spectroscopies. *Food Hydrocolloids* 13:35–41
- Kačuráková M, Capek P, Sasínikova V, Wellner N, Ebringerová A (2000) FT-IR study of plant cell wall model compounds: pectic polysaccharides and hemicelluloses. *Carbohydr Polym* 43:195–203
- Kataoka Y, Kiguchi M (2001) Depth profiling of photo-induced degradation in wood by FT-IR microspectroscopy. *J Wood Sci* 47:325–327
- Kataoka Y, Kondo T (1996) Changing cellulose crystalline structure in forming wood cell walls. *Macromolecules* 29:6356–6358
- Kataoka Y, Kondo T (1998) FT-IR microscopic analysis of changing cellulose crystalline structure during wood cell wall formation. *Macromolecules* 31:760–764
- Kataoka Y, Kiguchi M, Williams SR, Evans PD (2007) Violet light causes photodegradation of wood beyond the zone affected by ultraviolet radiation. *Holzforschung* 61:23–27
- Kim JS, Singh AP, Wi SG, Koch G, Kim YS (2008) Ultrastructural characteristics of cell wall disintegration of *Pinus* spp. in the windows of an old Buddhist temple exposed to natural weathering. *Int Biodeterior Biodegrad* 61(2):194–198
- Kleist G, Bauch J (2001) Cellular UV microspectrophotometric investigation of Sapelli heartwood (*Entandrophragma cylindricum* Sprague) from natural provenances in Africa. *Holzforschung* 55(2):117–122
- Kleist G, Schmitt U (2001) Characterisation of a soft rot-like decay pattern caused by *Coniophora puteana* (Schum.) Karst. in Sapelli wood (*Entandrophragma cylindricum* Sprague). *Holzforschung* 55(6):573–578
- Knorr F, Smith ZJ, Wachsmann-Hogiu S (2010) Development of a time-gated system for Raman spectroscopy of biological samples. *Opt Express* 18(19):20049–20058
- Koch G, Bauch J, Dunisch O, Seehann G, Schmitt U (1996) Secondary changes in wood of heavily stressed spruce (*Picea abies* L Karst) of high altitude stands of the east ore-mountains. *Holz Roh Werkst* 54(4):243–249
- Koch G, Rose B, Patt R, Kordsachia O (2003) Topochemical investigations on delignification of *Picea abies* L. Karst. during alkaline sulfite (ASA) and bisulfite pulping by scanning UV microspectrophotometry. *Holzforschung* 57(6):611–618
- Labbé N, Rials TG, Kelley SS, Cheng Z-M, Kim J-Y, Li Y (2005) FT-IR imaging and pyrolysis-molecular beam mass spectrometry: new tools to investigate wood tissues. *Wood Sci Technol* 39:61–77
- Lang L (1963) Absorption spectra in the ultraviolet and visible regions, vol 4. Academic Press, New York, p 84
- Larsen KL, Barsberg S (2010) Theoretical and Raman spectroscopic studies of phenolic lignin model monomers. *J Phys Chem B* 114(23):8009–8021
- Lehringer C, Gierlinger N, Koch G (2008) Topochemical investigation on tension wood fibres of *Acer* spp., *Fagus sylvatica* L. and *Quercus robur* L. *Holzforschung* 62(3):255–263
- Liang CY, Marchessault RH (1959a) Infrared spectra of crystalline polysaccharides. I. Hydrogen bonds in native celluloses. *J Polym Sci* 37:385–395
- Liang CY, Marchessault RH (1959b) Infrared spectra of crystalline polysaccharides. II. Native celluloses in the region from 640 to 1700  $\text{cm}^{-1}$ . *J Polym Sci* 39:269–278
- Marchessault RH (1962) Application of infra-red spectroscopy to cellulose and wood polysaccharides. *Pure Appl Chem* 5:107–129
- Matousek P, Towrie M, Stanley A, Parker AW (1999) Efficient rejection of fluorescence from Raman spectra using picosecond Kerr gating. *Appl Spectrosc* 53(12):1485–1489
- Matousek P, Towrie M, Ma C, Kwok WM, Phillips D, Toner WT, Parker AW (2001) Fluorescence suppression in resonance Raman spectroscopy using a high-performance picosecond Kerr gate. *J Raman Spectrosc* 32(12):983–988
- Morikawa Y, Yoshinaga A, Kamitakahara H, Wada M, Takabe K (2010) Cellular distribution of coniferin in differentiating xylem of *Chamaecyparis obtusa* as revealed by Raman microscopy. *Holzfor-schung* 64(1):61–67
- Müller G, Polle A (2009) Imaging of lignin and cellulose in hardwood using Fourier transform infrared microscopy—comparison of two methods. *NZ J Forest Sci* 39:225–231

- Musha Y, Goring DAI (1975) Distribution of Syringyl and Guaiacyl moieties in hardwoods as indicated by ultraviolet microscopy. *Wood Sci Technol* 9:45–58
- Naumann A, Polle A (2006) FTIR imaging as a new tool for cell wall analysis of wood. *NZ J Forest Sci* 36:54–59
- Nieduszynski I, Marchessault RH (1972) The crystalline structure of poly- $\beta$ , D(1–4')mannose: Mannan I. *Can J Chem* 50:2130
- Nuopponen M, Vuorinen T, Jamsa S, Viitaniemi P (2004) Thermal modifications in softwood studied by FT-IR and UV resonance Raman spectroscopies. *J Wood Chem Technol* 24(1):13–26
- Olsson A-M, Bjurhager I, Gerber L, Sundberg B, Salmén L (2011) Ultra-structural organisation of cell wall polymers in normal and tension wood of aspen revealed by polarisation FTIR microspectroscopy. *Planta* 233(6):1277–1286
- Osterberg M, Schmidt U, Jääskeläinen AS (2006) Combining confocal Raman spectroscopy and atomic force microscopy to study wood extractives on cellulose surfaces. *Colloid Surf A Physicochem Eng Asp* 291(1–3):197–201
- Pandey KK, Vuorinen T (2008) UV resonance Raman spectroscopic study of photodegradation of hardwood and softwood lignins by UV laser. *Holzforschung* 62(2):183–188
- Petry R, Schmitt M, Popp J (2003) Raman spectroscopy—a prospective tool in the life sciences. *Chem Phys Chem* 4(1):14–30
- Pew JC (1962) Biphenyl group in lignin. *Nature* 193:250–252
- Prislan P, Koch G, Cufar K, Gricar J, Schmitt U (2009) Topochemical investigations of cell walls in developing xylem of beech (*Fagus sylvatica* L.). *Holzforschung* 63(4):482–490
- Ruelle J, Yoshida M, Clair B, Thibaut B (2007) Peculiar tension wood structure in *Laetia procer* (Poep.) Eichl. (Flacourtiaceae). *Trees Struct Funct* 21(3):345–355
- Saariaho AM, Jääskeläinen AS, Nuopponen M, Vuorinen T (2003) Ultra violet resonance Raman spectroscopy in lignin analysis: Determination of characteristic vibrations of p-hydroxyphenyl, guaiacyl, and syringyl lignin structures. *Appl Spectrosc* 57(1):58–66
- Saariaho AM, Jaaskelainen AS, Matousek P, Towrie M, Parker AW, Vuorinen T (2004) Resonance Raman spectroscopy of highly fluorescing lignin containing chemical pulps: suppression of fluorescence with an optical Kerr gate. *Holzforschung* 58(1):82–90
- Saariaho A-M, Argyropoulos DS, Jääskeläinen A-S, Vuorinen T (2005) Development of the partial least squares models for the interpretation of the UV resonance Raman spectra of lignin model compounds. *Vib Spectrosc* 37(1):111–121
- Salmén L, Olsson A-M, Stevanic JS, Simonovic J, Radotic K (2012) Structural organisation of the wood polymers in the wood fibre structure. *Bioresources* 7(1):533–544
- Salzer R, Siesler HW (2009) Infrared and Raman spectroscopic imaging. Wiley, Weinheim
- Šašić S, Ozaki Y (2011) Raman, infrared, and near-infrared chemical imaging. Wiley, Hoboken
- Schmidt M, Gierlinger N, Schade U, Rogge T, Grunze M (2006) Polarized infrared microscopy of single spruce fibers: hydrogen bonding in wood polymers. *Biopolymers* 83:546–555
- Schmidt M, Schwartzberg AM, Perera PN, Weber-Bargioni A, Carroll A, Sarkar P, Bosneaga E, Urban JJ, Song J, Balakshin MY, Capanema EA, Auer M, Adams PD, Chiang VL, Schuck PJ (2009) Label-free in situ imaging of lignification in the cell wall of low lignin transgenic *Populus trichocarpa*. *Planta* 230(3):589–597
- Schmitt U, Grunwald C, Gricar J, Koch G, Cufar K (2003) Wall structure of terminal latewood tracheids of healthy and declining silver fir trees in the Dinaric region, Slovenia. *Iawa J* 24(1):41–51
- Schwanninger M, Rodrigues J, Pereira H, Hinterstoisser B (2004) Effects of short-time vibratory ball milling on the shape of FT-IR spectra of wood and cellulose. *Vib Spectrosc* 36(1):23–40
- Singh AP, Schmitt U, Möller R, Dawson BSW, Koch G (2006) Ray tracheids in *Pinus radiata* are more highly resistant to soft rot as compared to axial tracheids: relationship to lignin concentration. *Wood Sci Technol* 40:16–25
- Spurr AR (1969) A low-viscosity epoxy resin embedding medium for electron microscopy. *J Ultrastruct Res* 26(1–2):31. doi:10.1016/s0022-5320(69)90033-1
- Stadler J, Schmid T, Zenobi R (2010) nanoscale chemical imaging using top-illumination tip-enhanced Raman spectroscopy. *Nanoletters* 10:4514–4520
- Stevanic JS, Salmén L (2009) Orientation of the wood polymers in the cell wall of spruce wood fibres. *Holzforschung* 63:497–503
- Takayama M, Johjima T, Yamanaka T, Wariishi H, Tanaka H (1997) Fourier transform Raman assignment of guaiacyl and syringyl marker bands for lignin determination. *Spectrochimica Acta A* 53:1621–1628

- Tirumalai VC, Agarwal UP, Obst JR (1996) Heterogeneity of lignin concentration in cell corner middle lamella of white birch and black spruce. *Wood Sci Technol* 30(2):99–104
- Watanabe Y, Fukazawa K, Kojima Y, Funada R, Ona T, Asada T (1997) Histochemical study on heterogeneity of lignin in *Eucalyptus* species. 1. Effects of polyphenols. *Mokuzai Gakkaishi* 43(1):102–107
- Watanabe Y, Kojima Y, Ona T, Asada T, Sanol Y, Fukazawa K, Funada R (2004) Histochemical study on heterogeneity of lignin in *Eucalyptus* species II. The distribution of lignins and polyphenols in the walls of various cell types. *Iawa J* 25(3):283–295
- Wiley JH, Atalla RH (1987) Band assignments in the Raman-spectra of celluloses. *Carbohydr Res* 160:113–129
- Yin Y, Berglund L, Salmén L (2011) Effect of steam treatment on the properties of wood cell walls. *Biomacromolecules* 12:194–202
- Yoshida M, Ohta H, Okuyama T (2002) Tensile growth stress and lignin distribution in the cell walls of black locust (*Robinia pseudoacacia*). *J Wood Sci* 48(2):99–105
- Yoshida M, Fujiwara D, Tsuji Y, Fukushima K, Nakamura T, Okuyama T (2005) Ultraviolet microspectrophotometric investigation of the distribution of lignin in *Prunus jamasakura* differentiated on a three-dimensional clinostat. *J Wood Sci* 51(5):448–454
- Yoshinaga A, Fujita M, Saiki H (1997) Cellular distribution of guaiacyl and syringyl lignins within an annual ring in oak wood. *Mokuzai Gakkaishi* 43(5):384–390
- Yoshizawa N, Inami A, Miyake S, Ishiguri F, Yokota S (2000) Anatomy and lignin distribution of reaction wood in two *Magnolia* species. *Wood Sci Technol* 34(3):183–196